

# Frequency-selective self-trapping and supercontinuum generation in arrays of coupled nonlinear waveguides

I. Babushkin<sup>1</sup>, A. Husakou<sup>1</sup>, J. Herrmann<sup>1</sup>, and Yuri S. Kivshar<sup>2</sup>

<sup>1</sup>Max Born Institute for Nonlinear Optics and Short Pulse Spectroscopy, Max-Born-Street 2a, D-12489 Berlin, Germany

<sup>2</sup>Nonlinear Physics Center and Center for Ultra-high bandwidth Devices for Optical Systems (CUDOS), Research School of Physical Sciences and Engineering, Australian National University, Canberra ACT 0200, Australia

[ibabushkin@mbi-berlin.de](mailto:ibabushkin@mbi-berlin.de)

**Abstract:** We study spatiotemporal dynamics of soliton-induced two-octave-broad supercontinuum generated by fs pulses in an array of coupled nonlinear waveguides. We show that after fission of the input pulse into several fundamental solitons, red and blue-shifted nonsolitonic radiation, as well as solitons with lower intensity, spread away in transverse direction, while the most intense spikes self-trap into spatiotemporal discrete solitons.

© 2007 Optical Society of America

**OCIS codes:** (060.5530) Pulse propagation and solitons; (190.4420) Nonlinear optics, transverse effects in

---

## References and links

1. D. N. Christodoulides and R. I. Joseph, "Discrete self-focusing in nonlinear arrays of coupled waveguides," *Opt. Lett.* **13**, 794-796 (1988).
2. H. S. Eisenberg, Y. Silberberg, R. Morandotti, A. R. Boyd, and J. S. Aitchison, "Discrete spatial optical solitons in waveguide arrays," *Phys. Rev. Lett.* **81**, 3383-3386 (1998).
3. Yu. S. Kivshar, G. P. Agrawal, *Optical Solitons: from Fibers to Photonic Crystals* (Academic Press, San Diego, 2003).
4. D. N. Christodoulides, F. Lederer, and Y. Silberberg, "Discretizing light behaviour in linear and nonlinear waveguide lattices," *Nature* **424**, 817-823 (2003).
5. A. B. Aceves, C. De Angelis, A. M. Rubenchik, and S. K. Turitsyn, "Multidimensional solitons in fiber arrays," *Opt. Lett.* **19**, 329-331 (1994).
6. A. B. Aceves, G. G. Luther, C. De Angelis, A. M. Rubenchik, and S. K. Turitsyn, "Energy localization in nonlinear fiber arrays: Collapse-effect compressor," *Phys. Rev. Lett.* **75**, 73-76 (1995).
7. D. Cheskis, S. Bar-Ad, R. Morandotti, J. S. Aitchison, H. S. Eisenberg, Y. Silberberg, and D. Ross, "Strong spatiotemporal localization in a silica nonlinear waveguide array," *Phys. Rev. Lett.* **91**, 223901 (2003).
8. A. Yulin, D. V. Skryabin, and A. Vladimirov, "Modulational instability of discrete solitons in coupled waveguides with group velocity dispersion," *Opt. Express* **14**, 12347-12352 (2006), <http://www.opticsinfobase.org/abstract.cfm?URI=oe-14-25-12347>.
9. K. Motzek, A. A. Sukhorukov, and Yu. S. Kivshar, "Self-trapping of polychromatic light in nonlinear periodic photonic structures," *Opt. Express* **14**, 9873-9878 (2006), <http://www.opticsinfobase.org/abstract.cfm?URI=oe-14-21-9873>.
10. A. A. Sukhorukov, D. N. Neshev, A. Dreischuh, R. Fischer, S. Ha, W. Krolikowski, J. Bolger, A. Mitchell, B. J. Eggleton, and Yu. S. Kivshar, "Polychromatic nonlinear surface modes generated by supercontinuum light," *Opt. Express* **14**, 11265-11270 (2006), <http://www.opticsinfobase.org/abstract.cfm?URI=oe-14-23-11265>.
11. J. K. Ranka, R. S. Windeler, and A. J. Steinz, "Visible continuum generation in air silica microstructure optical fibers with anomalous dispersion at 800 nm," *Opt. Lett.* **25**, 25-27 (2000).
12. A. Husakou and J. Herrmann, "Supercontinuum generation of higher-order solitons by fission in photonic crystal fibers," *Phys. Rev. Lett.* **87**, 203901 (2001).

13. J. Herrmann, U. Griebner, N. Zhavoronkov, A. Husakou, D. Nickel, J. C. Knight, W. J. Wadsworth, and P. St. J. Russell, "Experimental evidence for supercontinuum generation by fission of higher-order solitons in photonic fibers," *Phys. Rev. Lett.* **88**, 173901 (2002).
14. W. H. Reeves, D. V. Skryabin, F. Biancalana, J. C. Knight, P. St. J. Russell, F. J. Omenetto, A. Efimov, A. J. Taylor, "Transformation and control of ultra-short pulses in dispersion-engineered photonic crystal fibers," *Nature* **424**, 511-515 (2003).
15. G. Genty, M. Lehtonen, and H. Ludvigsen, "Effect of cross-phase modulation on supercontinuum generated in microstructured fibers with sub-30 fs pulses," *Opt. Express* **12**, 4614-4624 (2004), <http://www.opticsinfobase.org/abstract.cfm?URI=oe-12-19-4614>.
16. A. V. Gorbach, D. V. Skryabin, J. M. Stone, and J. C. Knight, "Four-wave mixing of solitons with radiation and quasi-nondispersive wave packets at the short-wavelength edge of a supercontinuum," *Opt. Express* **14**, 9854-9863 (2006), <http://www.opticsinfobase.org/abstract.cfm?URI=oe-14-21-9854>.
17. J. M. Dudley, G. Genty, and S. Coen, "Supercontinuum generation in photonic crystal fiber," *Rev. Mod. Phys.* **78**, 1135-1184 (2006).
18. O. Fedotova, A. Husakou, and J. Herrmann, "Supercontinuum generation in planar rib waveguides enabled by anomalous dispersion," *Opt. Express* **14**, 1512-1517 (2006), <http://www.opticsinfobase.org/abstract.cfm?URI=oe-14-4-1512>.
19. M. J. Adams, *An Introduction to Optical Waveguides* (John Wiley & Sons, 1981).
20. A. Husakou and J. Herrmann, "Supercontinuum generation in photonic crystal fibers made from highly nonlinear glasses," *Appl. Phys. B* **77**, 227-234 (2003).
21. M. Frosz, P. Falk, and O. Bang, "The role of the second zero-dispersion wavelength in generation of supercontinua and bright-bright soliton-pairs across the zero-dispersion wavelength," *Opt. Express* **13**, 6181-6192 (2005) <http://www.opticsinfobase.org/abstract.cfm?URI=oe-13-16-6181>.

## 1. Introduction

Self-trapping of quasi-monochromatic beams in an array of coupled nonlinear waveguides and generation of spatial discrete solitons [1–4] have been studied extensively in recent years. However, an even more interesting case is the propagation of short pulses in arrays of nonlinear waveguides with anomalous dispersion. The discrete nature of the periodic array was predicted to support stable spatiotemporal solitons, in a sharp contrast to the collapse instability in the corresponding continuum structures [5–8]. The frequency-depending spatiotemporal dynamics of polychromatic light was investigated theoretically [9] and also experimentally [10], by studying the propagation of coherent supercontinuum light generated externally in a microstructure fiber in an array of LiNbO<sub>3</sub> waveguides with a photorefractive nonlinearity.

The discovery of supercontinuum (SC) in photonic crystal fibers with a width of more than one octave generated by fs pulses with nJ energy [11] has encouraged large research activities because of its many important applications. The SC generation with an input wavelength selected in the anomalous dispersion range is caused by the fission of the input pulse into several fundamental solitons which emit nonsolitonic radiation in a broad spectral range phase-matched to the corresponding solitons [12,13]. Besides, depending on the parameters of the system some additional effects, such as Raman soliton frequency shift, four-wave mixing and others can contribute to the resulting shape of supercontinuum (see [14–17] and references therein). Recently, it was shown that soliton-induced SC can also be generated in specifically designed planar rib waveguides [18].

In this paper, we study the nonlinear interaction and the mutual influence of the temporal dynamics of SC generation from fs input pulses and the self-focusing transverse dynamics in arrays of nonlinear waveguides. In contrast to the previous studies of polychromatic light self-focusing [9, 10], in our problem the SC radiation is not launched at the input of a waveguide array but it is generated in the array by fs pulses due to a fast Kerr-type nonlinear material itself. The presence of the linear coupling between the waveguides leads to a nontrivial modification of the spectral and temporal properties of the SC radiation in comparison to the SC generation in an isolated waveguide. We show that only the solitons with highest intensity become self-trapped into a *spatiotemporal discrete soliton*, while weaker solitons and nonsolitonic ra-

diation diffract into the neighboring waveguides. We predict that discrete diffraction provides an important mechanism of an intensity-depending and frequency-depending filtering.

## 2. Model and governing equations

We consider an array of planar rib waveguides with the geometry shown in Fig. 1(a) assuming that the waveguides are made of TaFD5 glass placed on SiO<sub>2</sub> substrate. Such waveguides exhibit an about 3 times larger nonlinear refractive index than for fused silica. For appropriate parameters the waveguide contribution to dispersion leads to a significant shift of the zero GVD wavelength to shorter wavelengths and anomalous dispersion in the visible, enabling the soliton-induced spectral broadening mechanism [18].

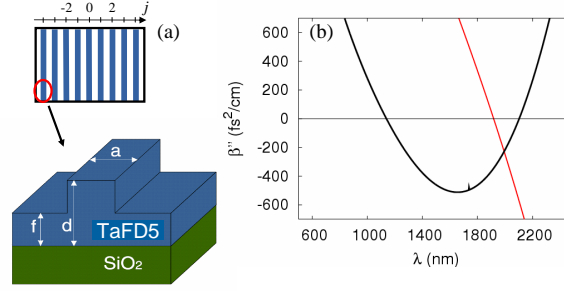


Fig. 1. (a) Schematic of a waveguide array created by planar rib waveguides. (b) Group-velocity dispersion for an Air-TaFD5-SiO<sub>2</sub> rib waveguide (black line) and bulk TaFD5 (red line). Waveguide dimensions are  $a = 4.0 \mu\text{m}$ ,  $d = 1.0 \mu\text{m}$ , and  $f = 0.5 \mu\text{m}$ .

We use a generalization of the forward Maxwell equation [12] for a waveguide array. This first-order equation is derived from the second-order wave equation neglecting the back-reflected wave but without the slowly-varying-envelope approximation. We suppose that all waveguides operate in the fundamental transverse  $E_{00}^x$  mode. The complex-valued Fourier transform  $\mathbf{E}_j(x, y, z, \omega)$  of the real-valued optical electric field  $\mathbf{E}_j(x, y, z, t)$  in the  $j$ -th waveguide can be written as  $E_j(z, \omega)\mathbf{F}(x, y, \omega)$ , where  $\mathbf{F}(x, y, \omega)$  is the transverse fundamental mode profile,  $z$  is the coordinate along the waveguides, whereas  $x$  and  $y$  are the transverse coordinates. Coupling between the waveguides in the array is assumed to be small, and it can be described in the tight-binding approximation [3]. The evolution of the Fourier transform of the field  $E_j \equiv E_j(z, \omega)$  along the  $z$  coordinate is then governed by the following equation:

$$i \frac{\partial E_j}{\partial z} + \left\{ \beta(\omega) - \frac{\omega}{v} \right\} E_j + \kappa (E_{j-1} + E_{j+1}) + \frac{\mu_0 \alpha(\omega) \omega^2}{2\beta(\omega)} P_{nl}^{(j)}(z, \omega) = 0. \quad (1)$$

Here  $\beta(\omega)$  is the propagation constant of the fundamental mode in the waveguide,  $\kappa$  is the coupling strength between the waveguides,  $P_{nl}^{(j)}(z, t) = \epsilon_0 \chi^{(3)} E_j^3(z, t)$  is the Kerr nonlinear polarization (without the Raman term for the case of TaFD5 glass),  $\alpha = \int |F|^4 dx dy / \int |F|^2 dx dy$  is the nonlinearity reduction factor,  $v$  is the velocity of the moving coordinate frame. The values of  $\beta(\omega)$  are calculated using the effective index approach [18, 19]. We notice that Eq. (1) is written directly for the electric field while the generalized nonlinear Schrödinger equation written for the complex amplitude is not numerically faster than Eq. (1) for the case of very broad spectra.

In Fig. 1(b), we show the GVD of a rib waveguide (black curve) with parameters specified in the figure caption, together with the GVD of bulk TaFD5 (red curve). The waveguide contribu-

tion to dispersion strongly shifts the zero-GVD wavelength to 1130 nm leading to a wide range of anomalous dispersion. The value  $\kappa = 6.25 \times 10^{-5} \mu\text{m}^{-1}$  of the linear coupling parameter between the waveguides corresponds to the waveguide separation about 10  $\mu\text{m}$ .

### 3. Numerical results and discussions

First, we study numerically the propagation of a relatively short (32 fs) input pulse with intensity of 0.5 TW/cm<sup>2</sup> and wavelength  $\lambda = 1600$  nm launched into the central ( $j = 0$ ) waveguide in an array of 11 coupled nonlinear waveguides. The chosen input intensity corresponds to an excitation of a third-order temporal soliton. For these parameters, in an isolated waveguide the input pulse splits into three fundamental solitons, seen in Fig. 2(a) as the three highest peaks, which emit weak nonsolitonic radiation (NSR), seen in Fig. 2(a) as weaker and longer leading or trailing pulses. For the waveguide parameters chosen here the GVD curve exhibits two zero-dispersion wavelengths [see Fig. 1(b)]. Previous studies of SC generation in photonic crystal fibers with two zero GVD points [18, 20, 21] predict that NSR is emitted both with shorter and longer wavelengths, which becomes separated in time due to walk-off. The same mechanism for the soliton-induced SC generation acts also in a waveguide array at the initial stage of the pulse evolution. However, as can be seen in Fig. 2(b), after propagation of 5 cm only the strongest soliton can resist the transverse spreading. The existence of *spatiotemporal discrete solitons* of such waveguide arrays was previously predicted theoretically [5, 6].

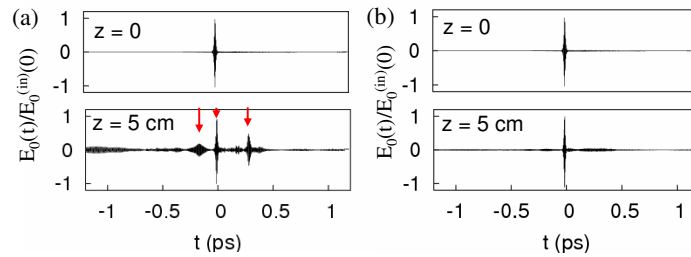


Fig. 2. Evolution of an input 32-fs pulse with peak intensity of 0.5 TW/cm<sup>2</sup> and central wavelength  $\lambda = 1600$  nm in an *isolated* waveguide (a) and the central waveguide of an array (b). Soliton fission appears both in (a) and (b), which leads to formation of three stable solitons in an isolated waveguide (marked by arrows), whereas only one most intense soliton resists diffractive spreading in the array.

In Fig. 3, we show both spectral and temporal characteristics for the central ( $j = 0$ ) and neighboring ( $j = 1$ ) waveguides by black ( $j = 0$ ) and red ( $j = 1$ ) curves, respectively. The strongest soliton at  $t = 0$  has a high intensity in the central waveguide, and it remains well-localized [Fig. 3(a)]. In contrast, the leading and trailing part of NSR is even stronger in the neighboring waveguide than in the central waveguide [cf. Fig. 3(a) and Fig. 3(b)]. Manifestation of this effect in the spectral domain is illustrated by Fig. 3(c). Comparison of the spectra in the central (black curve) and neighboring (red curve) waveguides shows spreading for the spectral components around 700 nm and 2700 nm, which correspond to the blue- and red-shifted NSR. In contrast, the spectral part around 1500 nm, which corresponds to the soliton spectrum, is highly localized in the central waveguide [black curve in Fig. 3(c)] and only a very weak part is coupled into the  $j = 1$  waveguide. We call this effect *frequency-selective self-trapping*, whereby the selection of distinct spectral parts is related to the soliton dynamics and the emission of NSR by solitons. As a measure for the pulse localization in the waveguide array we use the spectrally resolved quadratic mean of the mode diameter of the pulse  $W_{\text{RMS}}(\omega) = [\sum_j j^2 I_j(\omega) / \sum_j I_j(\omega)]^{1/2}$ , where

$I_j(\omega)$  is the spectral power in the  $j$ -th waveguide. This quantity, depicted in Fig. 3(d), clearly shows the above-mentioned frequency-dependent trapping.

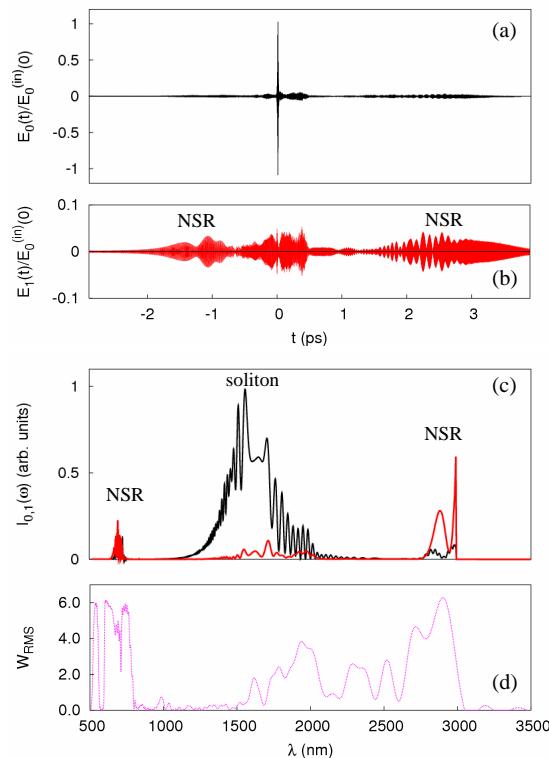


Fig. 3. (a,b) Temporal profile and (c) spectrum of pulse in the central [black curve in (a,c)] and neighboring [red curve in (b,c)] waveguide. Parameters of the input pulse are the same as in Fig. 2(b), propagation length is 5 cm. (d) Quadratic mean of the mode diameter  $W_{RMS}(\omega)$  characterizing the field localization. Nonsolitonic radiation (NSR) and soliton are separated both in (a,b) temporal and (c) spectral domains.

The spectrum of the  $N = 3$  soliton is still relatively narrow [Fig. 3(c)]. Now we study the evolution for a longer input pulse (200 fs) with the same intensity corresponding to the soliton number of about  $N = 20$ , as shown in Fig. 4 by the temporal profile with many soliton spikes and NSR [Fig. 4(b)] and a two-octave spectrum extending from 500 to 3000 nm [Fig. 4(a)]. After 5 cm propagation in the waveguide array, SC is generated in the central waveguide being of the same width and similar shape, as shown in Fig. 4(c) (black curve). A comparison between black and red curves in Fig. 4(c,d) reveals that NSR around 700 nm and 2700 nm is coupled to the neighboring waveguide while the soliton spikes remain self-trapped in the central waveguide, thus demonstrating the frequency-selective self-trapping similar to the short-pulse case. For larger propagation distance [Fig. 4(e,f)], only the strongest spike remains in the central waveguide, and forms a spatiotemporal discrete soliton.

For comparison, we consider also the regime of normal GVD and the input wavelength of 800 nm, illustrated in Fig. 5. For normal GVD solitons can not be generated and, therefore, the pulse does not split but is reshaped towards a top-hat profile [black curve in Fig. 5(b)] and spectral broadening by self-phase modulation yields a much narrower spectrum as can be seen in Fig. 5(a). Therefore, the transverse diffraction occurs equally for all time positions and

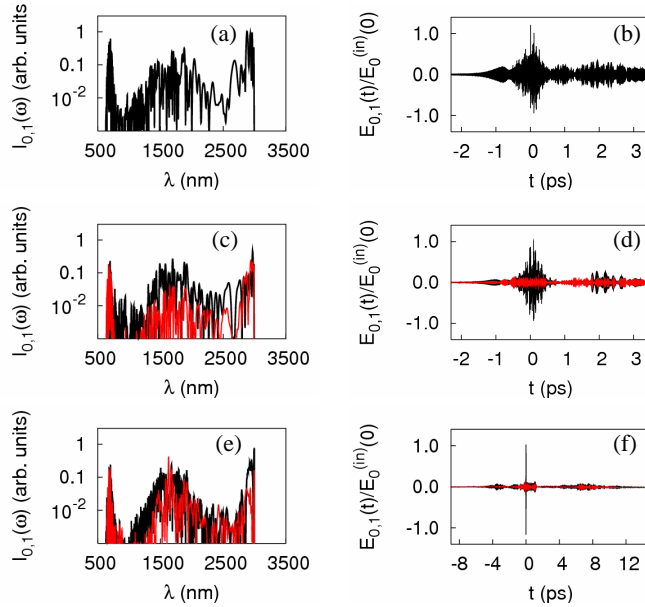


Fig. 4. (a,c,e) Spectrum and (b,d,f) temporal shape calculated for a 200 fs input pulse with peak intensity  $0.5 \text{ TW/cm}^2$  and central wavelength 1600 nm in (a,b) an isolated waveguide and (c-f) waveguide array. Propagation length is (a-d) 5 cm and (e,f) 20 cm, respectively.

spectral components, as can be seen in Fig. 5. In this case, for a large enough propagation distance the transverse discrete diffraction destroys the localization of the whole pulse.

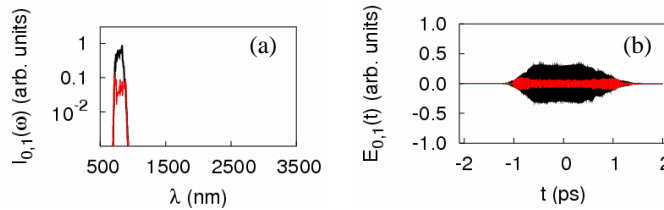


Fig. 5. (a) Spectrum and (b) temporal shape calculated for a 200-fs input pulse with peak intensity  $0.5 \text{ TW/cm}^2$  and central wavelength 800 nm propagating for  $z = 5 \text{ cm}$ .

#### 4. Conclusions

We have analyzed supercontinuum generation and frequency-selective self-trapping of femtosecond pulses in nonlinear waveguide arrays with fast Kerr nonlinearity and anomalous dispersion. The effects observed can be related to fission of the input pulse into several fundamental solitons and weak blue- and red-shifted nonsolitonic radiation. The most intense central part of the spectrum is self-trapped and forms with further propagation spatiotemporal discrete solitons. Weaker radiation becomes separated in time from the main part of the pulse, and cannot be self-trapped anymore. We demonstrate that, for large enough duration of the input pulse, more than two octaves broad supercontinuum can be generated in the waveguide array.